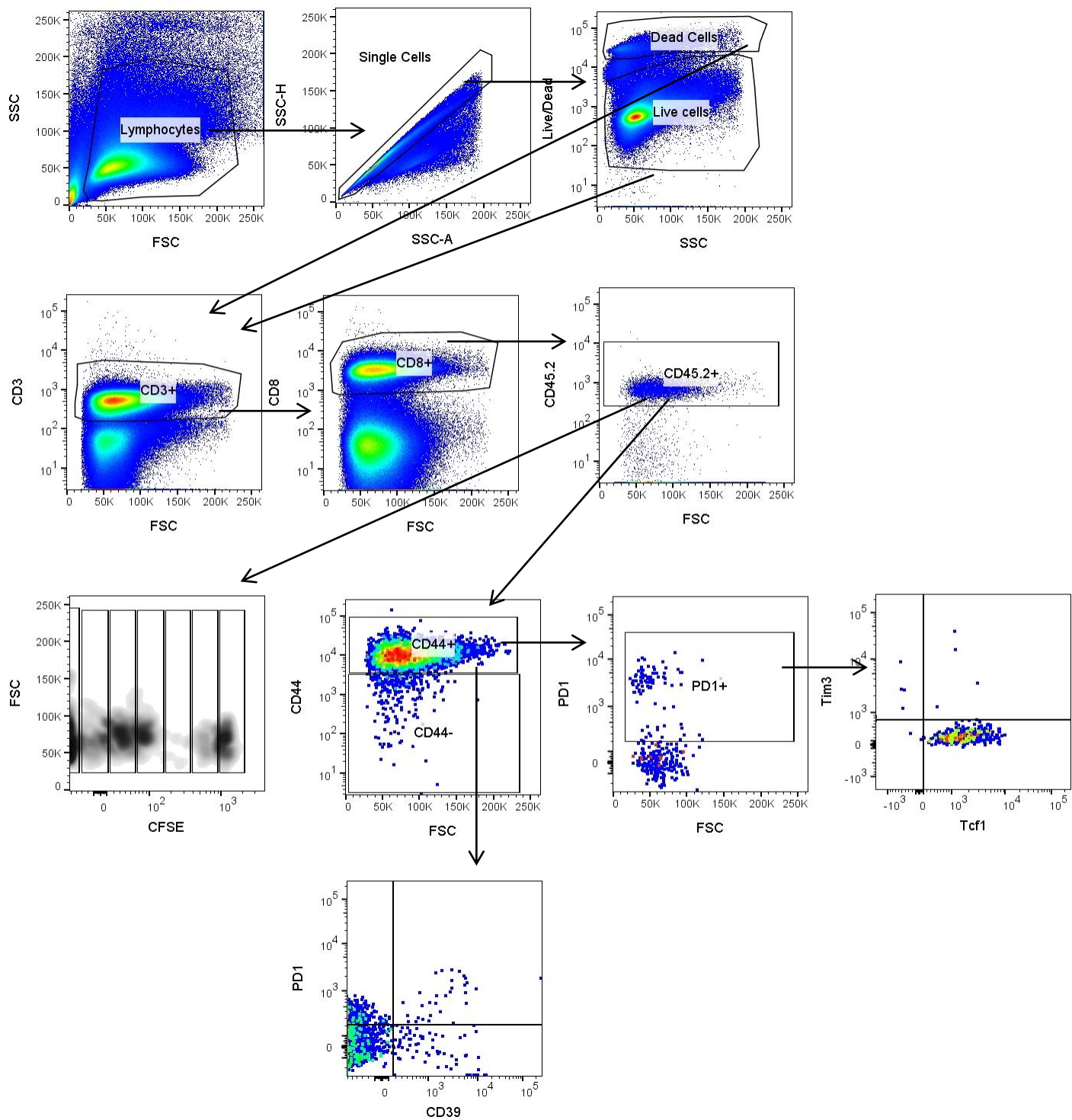
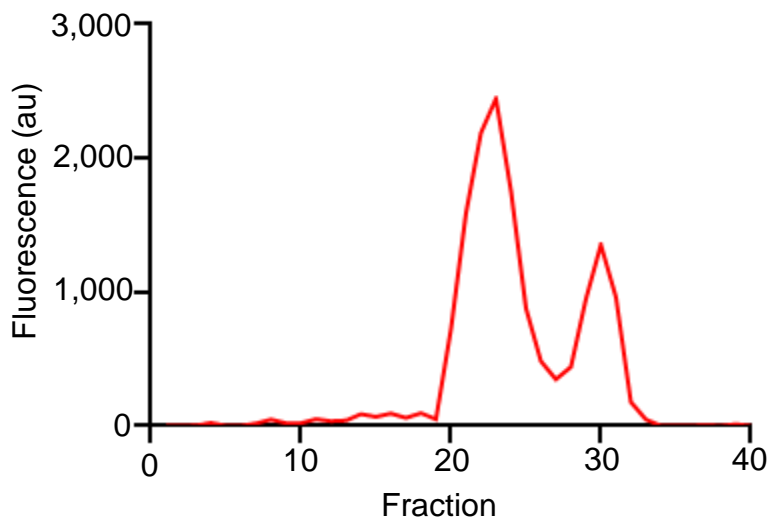


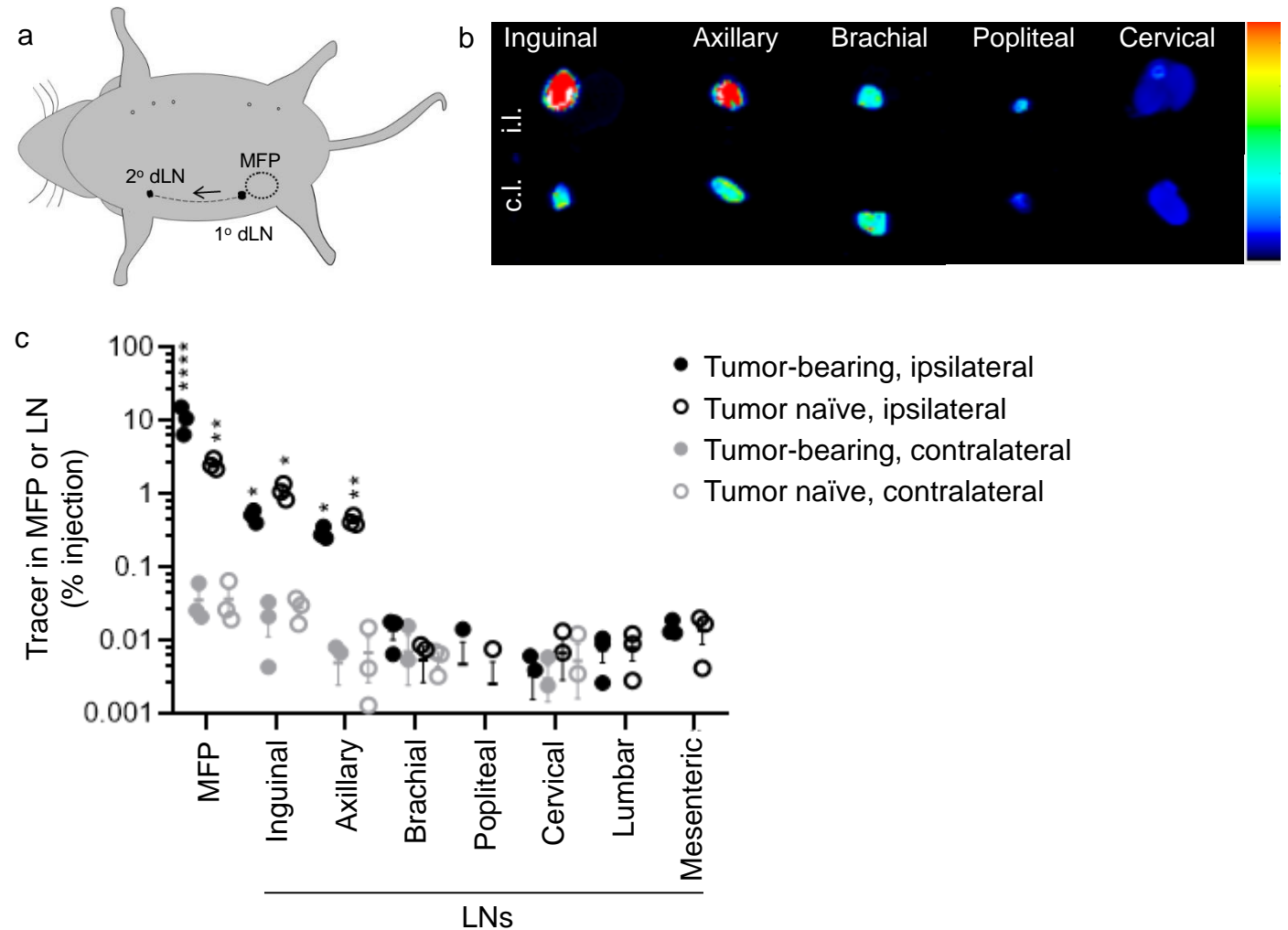
**Supplemental Figure 1** Viability, purity, and CFSE loading of isolated CD8+ OT-I donor cells prior to transfer into CD45.1 recipient animals



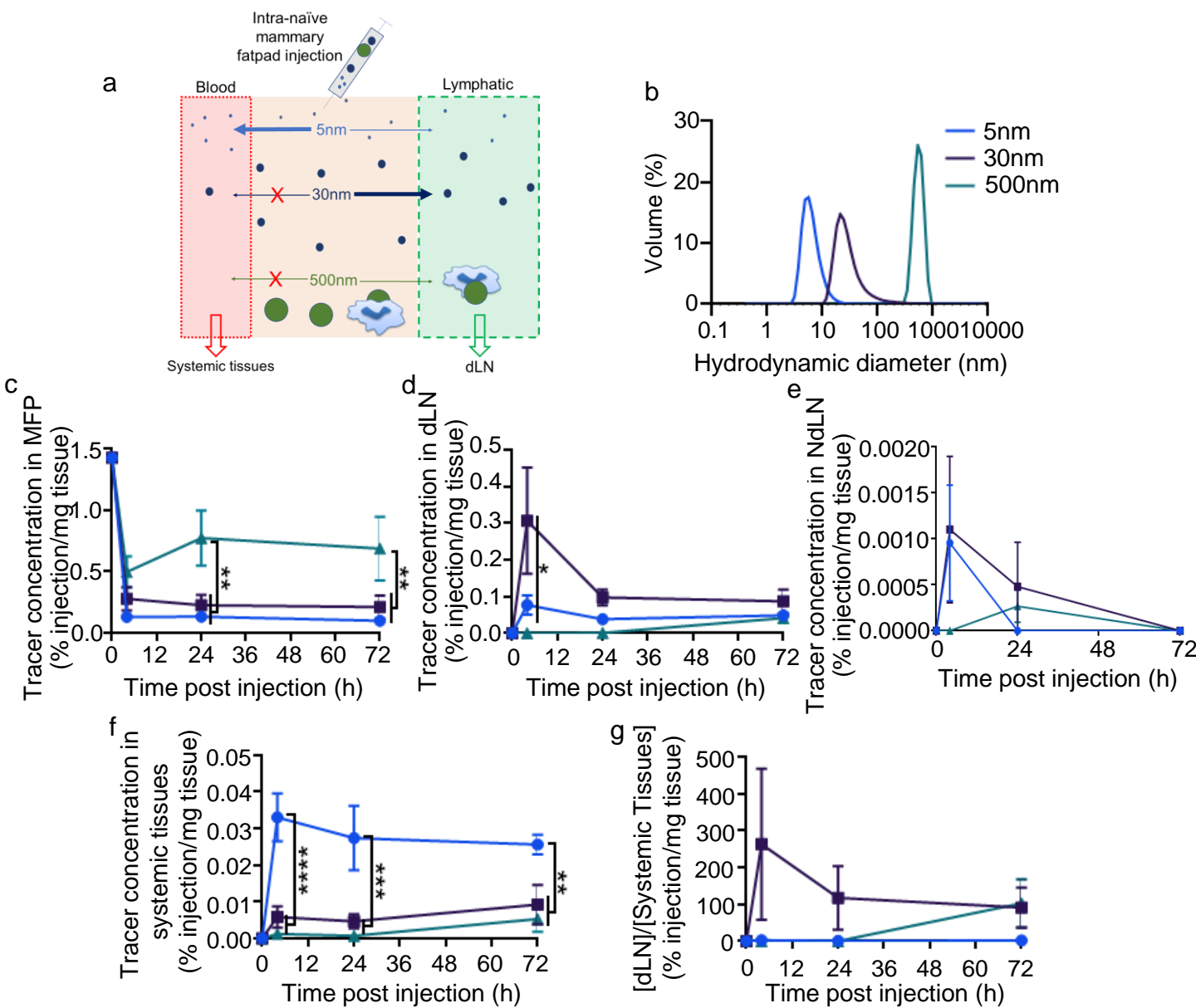
**Supplemental Figure 2** Flow cytometry gating for adoptive transfer experiments, from an example LN analyzed 96 hours after transfer into a day 7 tumor.



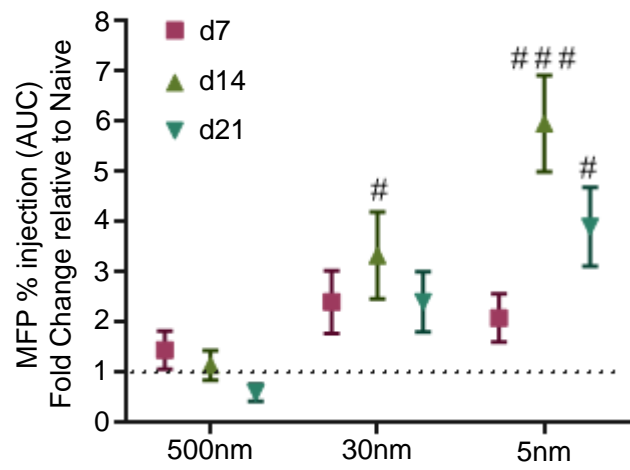
**Supplemental Figure 3** Size exclusion chromatography showing separation of fluorescently labelled 30nm dextran from free AF700 dye



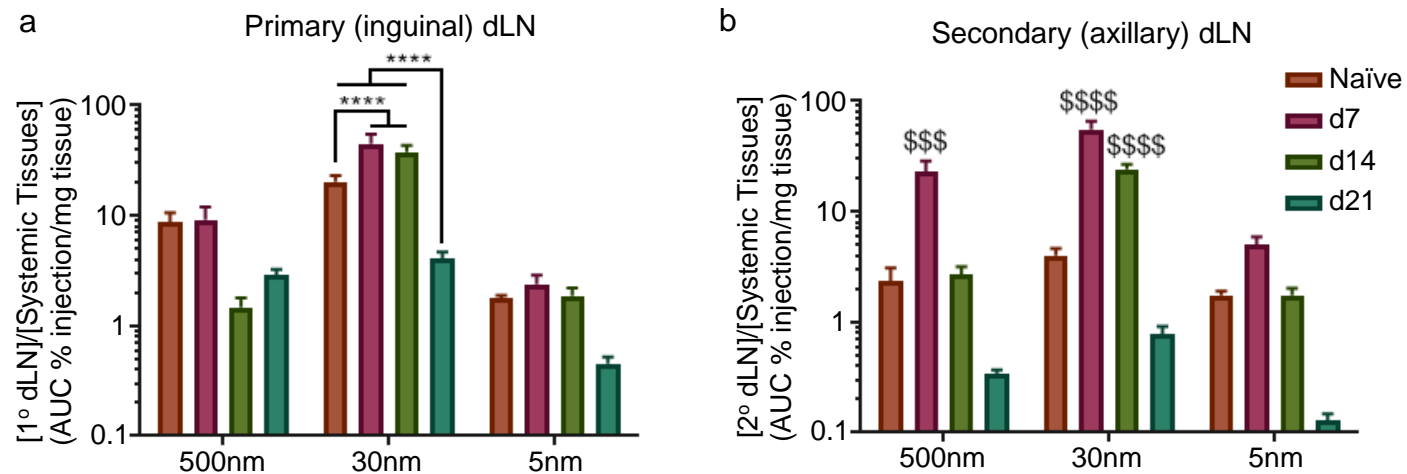
**Supplemental Figure 4** Lymph node mapping in naïve and day 11 E0771-bearing animals. **(a)** Schematic showing approximate locations of fourth (inguinal) MFP [location of tumor implantation], dLNs (inguinal and axillary), and contralateral nipples as reference points. **(b)** IVIS images of excised draining (ipsilateral) and non-draining (contralateral) inguinal, axillary, brachial, popliteal, and cervical LNs 24 h after injection of AF647-labelled 500kDa (30nm) dextran into MFP. **(c)** Quantification of AF647-labelled 500kDa (30nm) dextran accumulation 24 h after injection into the naïve MFP or d11 tumor in homogenates of each of 7 LNs and the mammary fatpad (MFP), including both the tissue ipsilateral and contralateral to the site of injection (with the exception of the lumbar and mesenteric LNs, for which there is no contralateral tissue). \* indicates significance relative to contralateral side by t-test; n=3 animals



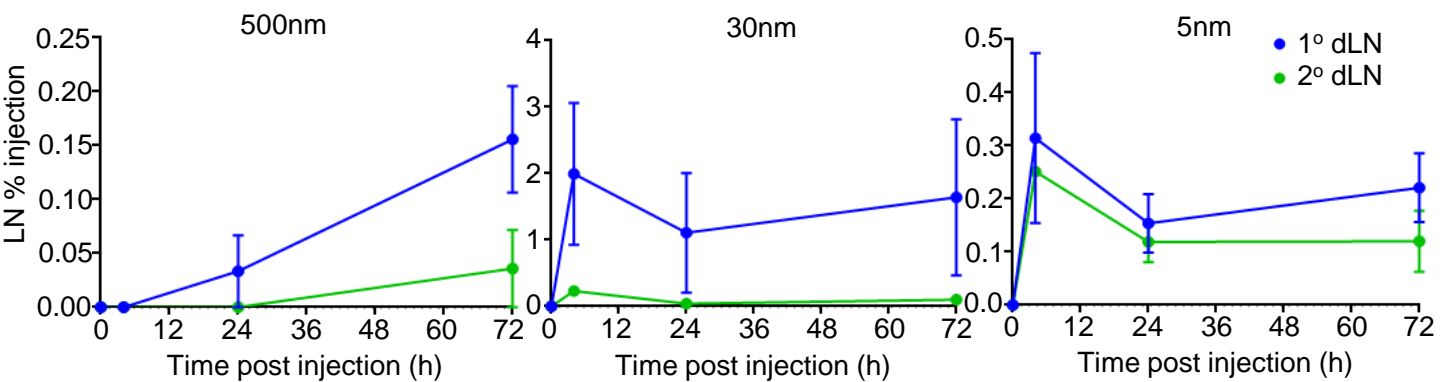
**Supplemental Figure 5** Dynamics of macromolecular distribution from the mammary fatpad is size-dependent. **(a)** Schematic of molecular clearance routes from the intra-mammary fatpad. **(b)** Dynamic light scattering tracer measurements. **(c)** Tracer retention at the mammary fatpad injection site over 72 h. **(d-f)** Tracer accumulation within draining (c) and non-draining (d) LN and spleen, liver, lungs, kidneys (f) over 72 h post injection in the mammary fatpad. **(g)** Relative tracer concentration within dLN compared to systemic tissues (liver, lungs, spleen, and kidneys) from 0-72 h. \* indicates significance by two-way ANOVA with Tukey comparison; n=5-6 mice



**Supplemental Figure 6** Fold change in tracer retention at injection site resulting from tumor formation and growth over 72 h post injection quantified as % injection AUC. # indicates significance by one-sample t-test relative to theoretical value of 1.0; n=5-6 mice

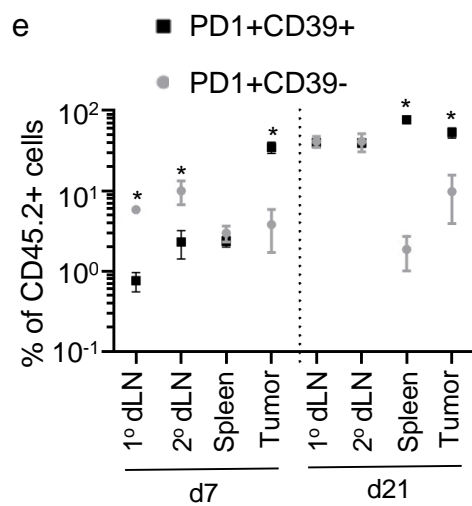
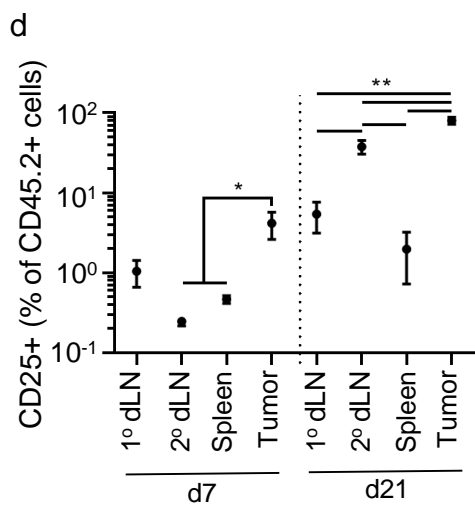
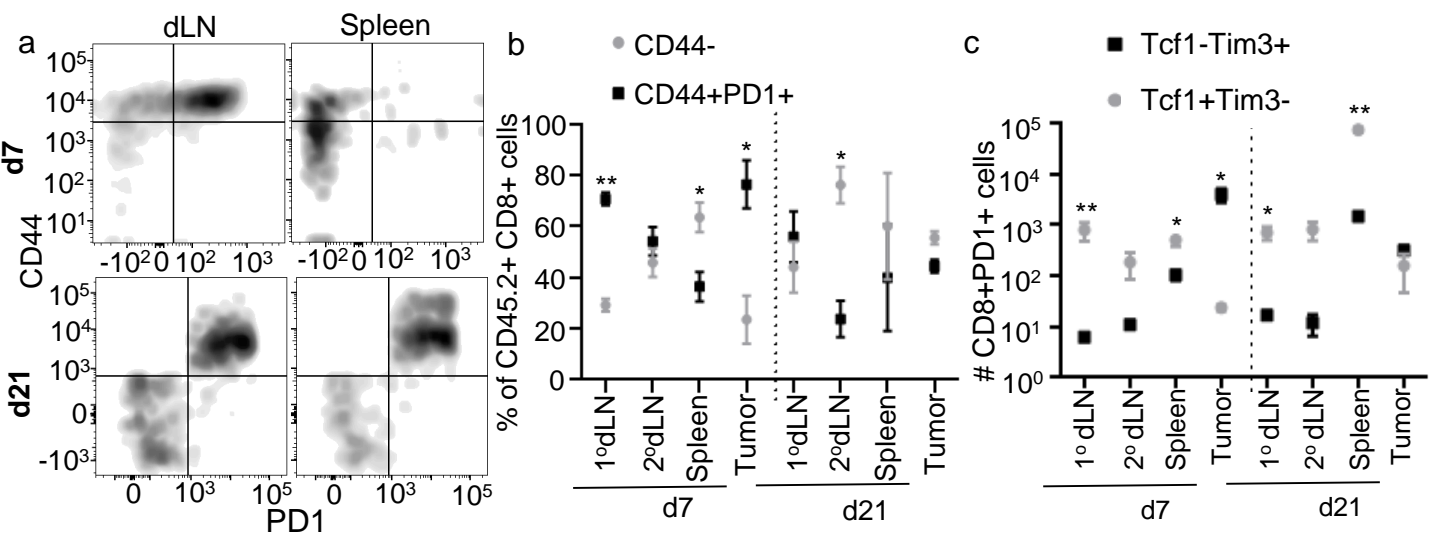


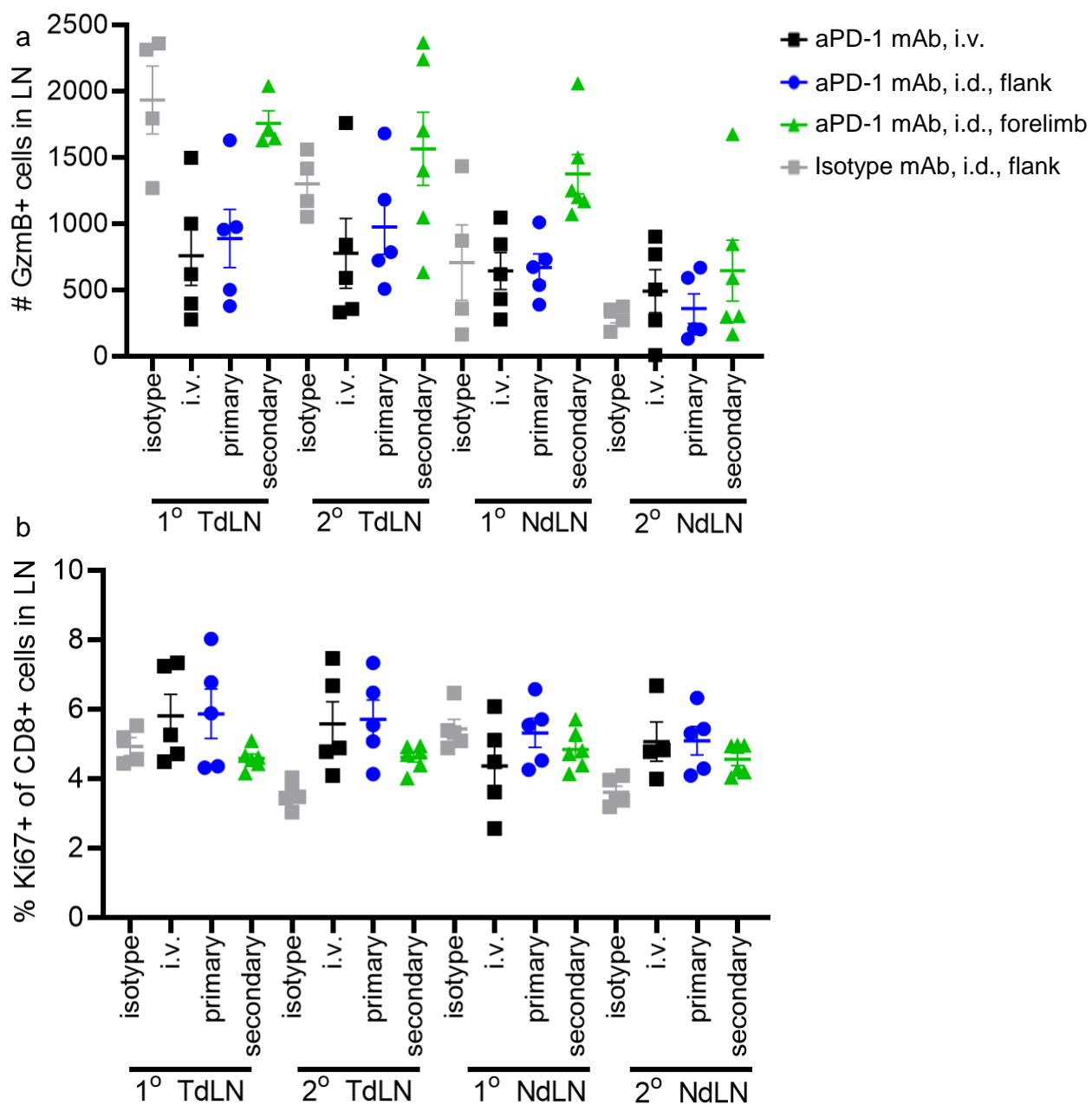
**Supplementary Figure 7** Ratio of tracer concentrations within primary (**a**) and secondary (**b**) dLNs relative to systemic tissues (liver, kidneys, spleen, lungs) of 72 h post injection the mammary fatpad of naïve or E0771 tumor bearing animals at different stages of disease as quantified by concentration AUC. \* indicates significance by two-way ANOVA with Tukey's post-hoc test; \$ indicates significance relative to all other groups by two-way ANOVA with Tukey's post-hoc test; n=5-6 mice



**Supplemental Figure 8** Levels of tracer accumulation in primary and secondary dLNs over 72 h post injection in the mammary fatpad. n=5-6 mice.







**Supplemental Figure 9** Granzyme B (a) and Ki67 (b) expression by CD8+ T cells within tumor draining- and non-draining primary and secondary LNs after aPD-1 administration i.v., i.d. in the flank, or i.d. in the forelimb compared to isotype mAb administered in the flank. One-way ANOVA with Tukey's comparison revealed no significance between groups in either readout. n=5-6 mice